

## Asymmetric fission barriers and total kinetic energies for $^{194}\text{Hg}$ , $^{149}\text{Tb}$ , $^{110-112}\text{In}$ , $^{94}\text{Mo}$ , and $^{75}\text{Br}$

G. Royer and F. Haddad

*Laboratoire de Physique Subatomique et des Technologies Associées "Subatech,"  
UMR:IN2P3/CNRS-Université-Ecole des Mines, 2 rue de la Houssinière, 44072 Nantes Cedex 03, France*

(Received 5 December 1994)

The asymmetric fission barriers and the released kinetic energies in the deformation valley leading rapidly to two tangent spherical fragments have been calculated for  $^{194}\text{Hg}$ ,  $^{149}\text{Tb}$ ,  $^{110-112}\text{In}$ ,  $^{94}\text{Mo}$ , and  $^{75}\text{Br}$  within the generalized liquid-drop model including the nuclear proximity energy. Results are compared to experimental data and predictions of the Yukawa plus exponential finite range liquid-drop model and the liquid-drop model. The calculated asymmetric fission barrier heights lie between the values obtained by the two other theoretical approaches.

PACS number(s): 24.75.+i, 25.85.-w

Light nuclei decay primarily by light-particle emission since the macroscopic fission barrier heights increase monotonically with the fragment symmetry. For heavier nuclei, the macroscopic symmetric fission barrier is lower than the macroscopic asymmetric fission barrier except for the greatest asymmetries corresponding to the light-particle evaporation and for the actinides for which shell effects play the major role. Therefore, the major nuclear decay modes are symmetric fission and light-particle emission. Nevertheless, heavy-ion reactions have allowed one to explore an asymmetric binary fissionlike breakup from central collisions at low to intermediate energies. Excitation functions and kinetic energies of the intermediate mass fragments are now available and asymmetric fission barrier heights can be extracted [1-8]. These data allow one to test the ability of the current macroscopic nuclear models to describe the symmetric fission, the intermediate mass fragment production, and the light-particle emission as a common process only governed by the mass-asymmetry coordinate.

In previous works [9-11] the fusionlike second fission valley has been investigated within a generalized liquid-drop model including the nuclear proximity energy. This peculiar deformation path is plausible since the potential barrier heights correspond roughly to the experimental fission barrier heights in the whole mass range when the effects of the nuclear proximity forces between the nascent fragments are properly taken into account.

The purpose of the present work is, first, to study the compatibility of this deformation valley described within our macroscopic approach with recent experimental data relative to fission barriers and total kinetic energies for very asymmetric breakup and, second, to compare (for some results) with predictions of the Yukawa plus exponential finite-range liquid-drop model (YEFRLDM [12,13]) and the liquid-drop model (LDM, [14]). The differences between these three macroscopic approaches lie both in the selected shape sequences and in the chosen ingredients to determine the potential energy. The YEFRLDM and LDM rather explore elongated shapes with shallow and wide necks. In contrast, to maximize and test the influence of the proximity energy during the splitting of the nucleus, we have defined [9,15] a sequence

of compact and creviced shapes describing the rapid formation of a deep and narrow neck leading the initial nucleus to two tangent unequal spherical fragments which go away later. Then the saddle point corresponds to two separated fragments maintained in equilibrium by the balance between the attractive proximity forces and the repulsive Coulomb forces, except for the largest asymmetries for which the saddle point stands close to the sphere just before the neck development.

Within our approach derived from the generalized liquid-drop model, the energy of the deformed nucleus is given by [15]

$$E = -a_V(1 - k_V I^2)A + a_S(1 - k_S I^2)A^{2/3}(S/4\pi R_0^2) + \frac{3}{5}e^2 \frac{Z^2}{R_0} B_c + E_{\text{prox}} \quad (1)$$

$A$ ,  $Z$ , and  $I = (N - Z)/A$  are the mass, charge, and relative neutron excess of the initial nucleus. The surface energy coefficient  $a_S$  and the surface asymmetry coefficient  $k_S$  are taken as

$$a_S = 17.9439 \text{ MeV} \quad \text{and} \quad k_S = 2.6 \quad (2)$$

The volume energy coefficient  $a_V$  and the volume asymmetry coefficient  $k_V$  take on the values

$$a_V = 15.494 \text{ MeV} \quad \text{and} \quad k_V = 1.8 \quad (3)$$

$B_c$  is the Coulomb shape-dependent function calculated from elliptic integrals. The effective sharp radius is defined by

$$R_0 = 1.28A^{1/3} - 0.76 + 0.8A^{-1/3} \text{ fm} \quad (4)$$

$R_0/A^{1/3}$  equals 1.13 fm for  $^{40}\text{Ca}$  and 1.18 fm for  $^{240}\text{Pu}$ . When the two fragments are separated the volume, surface, and Coulomb energies are, respectively, given by

$$E_V = -a_V[(1 - k_V I_1^2)A_1 + (1 - k_V I_2^2)A_2] \quad (5)$$

$$E_S = a_S[(1 - k_S I_1^2)A_1^{2/3} + (1 - k_S I_2^2)A_2^{2/3}] \quad (6)$$

$$E_C = \frac{3}{5}e^2 Z_1^2/R_1 + \frac{3}{5}e^2 Z_2^2/R_2 + e^2 Z_1 Z_2/r \quad (7)$$

All along the fission path, the nuclear proximity energy which takes into account the finite-range effects of the nucleon-nucleon force inside the crevice or the gap separating the two nascent fragments reads

$$E_{\text{prox}} = 2\gamma \int \phi[D(h)/b]2\pi h dh \quad (8)$$

with

$$\gamma = 0.9517 \sqrt{(1 - k_s I_1^2)(1 - k_s I_2^2)} \text{ MeV fm}^{-2} . \quad (9)$$

$h$  is the transverse distance varying from the neck radius to the height of the neck border (see Fig. 1).  $D$  is the distance between the opposite infinitesimal surfaces,  $b = 0.99$  fm is the surface width, and  $\phi$  is the proximity function.

The discontinuity of a few MeV appearing at the contact point due to the difference between  $Z_1/A_1$  and  $Z_2/A_2$  has been linearized from the sphere to the contact point supposing that the charge rearrangement occurs progressively. For comparison, the LDM [14] does not take into account the proximity energy and assumes

$$a_S = 17.9439 \text{ MeV} , \\ R_0/A^{1/3} = 1.2249 \text{ fm} ,$$

and

$$k_S = 1.7826 . \quad (10)$$

The adopted equation (4) allows one to lower significantly the nuclear radius and to detail its mass dependence.

The values of the constants used in the YEFRLDM are, respectively,

$$a_S = 21.13 \text{ MeV} , \\ R_0/A^{1/3} = 1.16 \text{ fm} ,$$

and

$$k_S = 2.3 . \quad (11)$$

The essential difference resides in the value of the surface energy coefficient  $a_S$ . There is still a large incertitude on these coefficients [13,16].

In Fig. 2 recent data on the asymmetric breakup of the  $^{149}\text{Tb}$  compound nucleus obtained in the  $^{86}\text{Kr} + ^{63}\text{Cu}$  reaction are compared with calculations. It is known

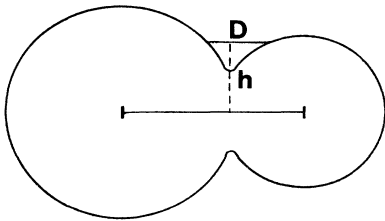


FIG. 1. Schematic definition of the height  $h$  and the corresponding distance  $D$  in the neck.

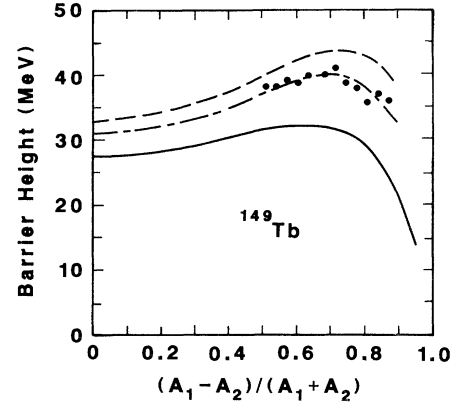


FIG. 2. Comparison of experimental and theoretical fission barrier heights for  $^{149}\text{Tb}$  as functions of the fission asymmetry. The experimental data are taken from [7]. The solid and dashed lines correspond, respectively, to the YEFRLDM [12,13] and LDM [14] predictions while our results are given by the dashed-dotted curve.

that the LDM predicts too high fission barrier heights for light and mass intermediate nuclei. Here, the difference with the data is only 10%. In contrast, the experimental barriers are 37% greater than those determined by the YEFRLDM which, nevertheless, reproduces generally accurately nuclear masses and fission and fusion barrier heights. Our prediction agrees well with the data. In Fig. 3, the same comparison is done for  $^{75}\text{Br}$ . The experi-

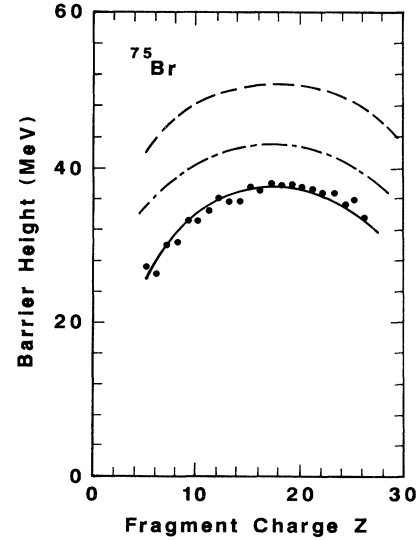


FIG. 3. Comparison of experimental and theoretical fission barrier heights for  $^{75}\text{Br}$  as functions of the fragment charge. The experimental data are taken from [5]. The solid and dashed curves give, respectively, the YEFRLDM and LDM predictions. The dash-dotted curve corresponds to our results.

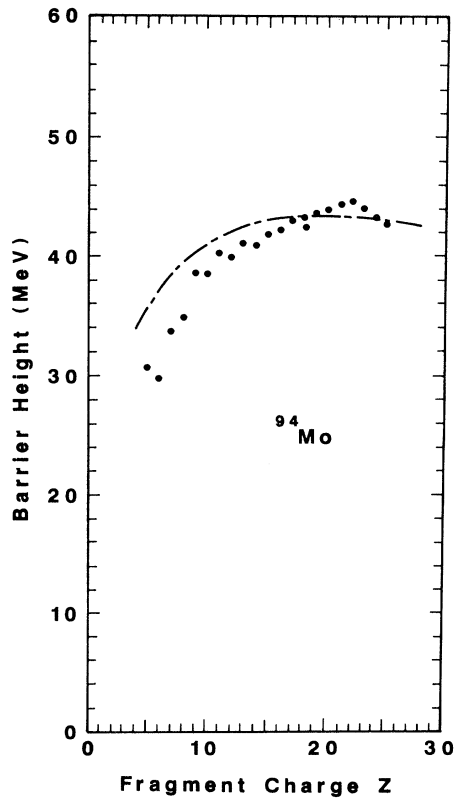


FIG. 4. Comparison of experimental asymmetric fission barrier heights [8] and our predictions (dash-dotted curve) for  $^{94}\text{Mo}$ .

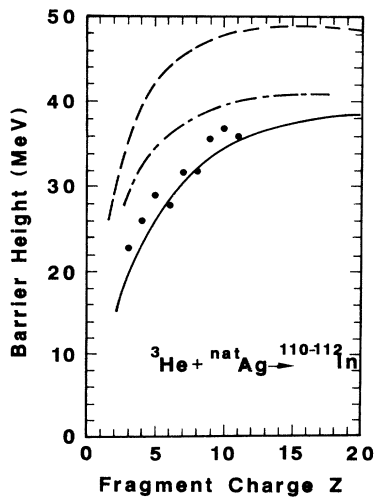


FIG. 5. Same as Fig. 3 but for the In nucleus. The experimental data are taken from [2].

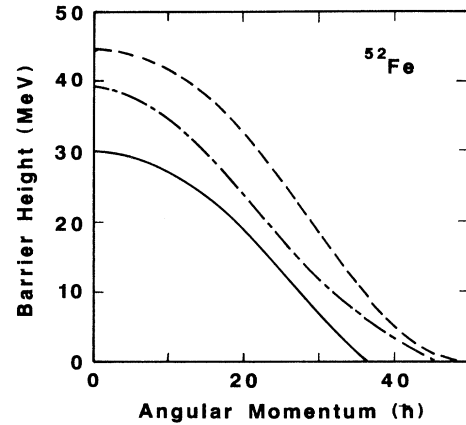


FIG. 6. Comparison of theoretical fission barrier heights (see [4]) vs angular momentum for the  $^{52}\text{Fe}$  light nucleus determined from the rotating liquid-drop model (dashed line), the Yukawa plus exponential finite-range model (solid line), and our approach (dash-dotted line).

mental results coincide with the YEFRLDM calculations while the two other approaches lead to too high barriers. The data seem somewhat uncertain since Boger and Alexander [7] note that  $^4\text{He}$  emission was not considered in the analysis though its cross sections are known to be important. Figures 4 and 5 show that our approach reproduces also fairly well the recent data for  $^{94}\text{Mo}$  (except for the lightest fragments) while it overestimates slightly the barriers for the In nucleus. In all cases, our asymmetric fission barrier heights lie between the predictions of the LDM and YEFRLDM models. Figure 6 indicates

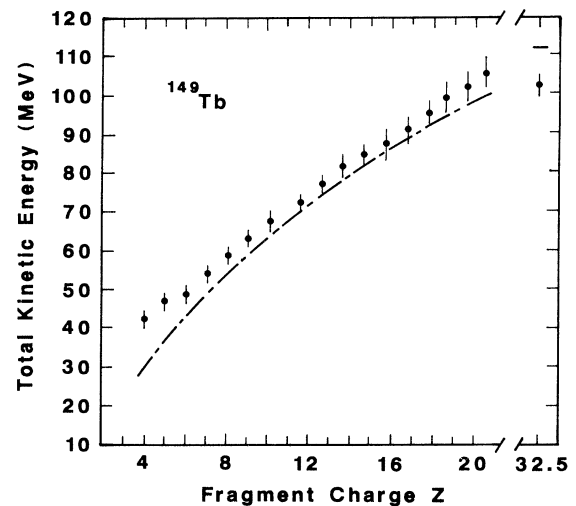


FIG. 7. Fission total kinetic energies as a function of the light fragment charge for  $^{149}\text{Tb}$ . The theoretical estimate is based upon the energy at the scission point defined by  $|E_{\text{prox}}| < 0.5$  MeV. The experimental data are extracted from [6].

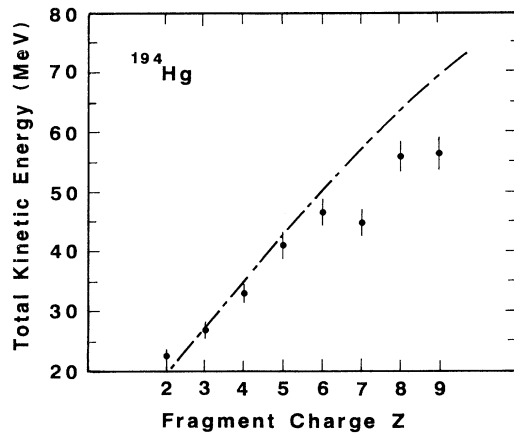


FIG. 8. Comparison between experimental TKE's [1,3] and our predictions (dash-dotted curve) for light fragment emission from  $^{194}\text{Hg}$ .

that this result is also valid in the symmetric fission case for light nuclei. For heavier nuclei, the YEFRLDM and our approach lead to about the same symmetric fission barrier heights [9] but the calculated maximal angular

momentum against fission is higher in the deformation path through compact and creviced shapes due to the position of the saddle point and the curvature at the top of the barrier [9,11].

The total kinetic energy (TKE) of the fragments is the potential energy at the scission point plus the possible prescission kinetic energy. In this second fission valley, the scission point is not the point where the rupture of the matter bridge between the future fragments occurs since the barrier top is not still reached. The effective scission point is more external and lower than the saddle point and corresponds, on the potential barrier, to the position where the proximity forces end to act. In Figs. 7 and 8, the TKE's of the intermediate mass fragments produced during the asymmetric fission of  $^{149}\text{Tb}$  and  $^{194}\text{Hg}$  are displayed. Our predictions agree nicely with the measured values in the first case but there are some discrepancies with the data relative to  $^{194}\text{Hg}$ .

Finally, it seems that the very asymmetric fission leading to intermediate mass fragments may be described within the hypothesis that spherical fragments are rapidly emitted by compact nuclei and that the basic ideas of the liquid-drop model are still valid if the proximity energy is taken into account.

- 
- [1] L. C. Vaz, D. Logan, J. M. Alexander, E. Duek, D. Guerreau, L. Kowalski, M. F. Rivet, and M. S. Zisman, *Z. Phys. A* **311**, 89 (1983).
- [2] M. A. McMahan, L. G. Moretto, M. L. Padgett, G. J. Wozniak, L. G. Sobotka, and M. G. Mustafa, *Phys. Rev. Lett.* **54**, 1995 (1985).
- [3] N. Carjan and J. M. Alexander, *Phys. Rev. C* **38**, 1692 (1988).
- [4] K. Grotowski, R. Planeta, M. Blann, and T. Komoto, *Phys. Rev. C* **39**, 1320 (1989).
- [5] D. N. Delis, Y. Blumenfeld, D. R. Bowman, N. Colonna, K. Hanold, K. Jing, M. Justice, J. C. Meng, G. F. Peaslee, G. J. Wozniak, and L. G. Moretto, *Z. Phys. A* **339**, 279 (1991).
- [6] N. Carjan and M. Kaplan, *Phys. Rev. C* **45**, 2185 (1992).
- [7] J. Boger and J. M. Alexander, *Phys. Rev. C* **50**, 1006 (1994).
- [8] L. G. Moretto, K. X. Jing, and G. J. Wozniak, Lawrence Berkeley Laboratory Report No. 36186, 1994 (unpublished).
- [9] G. Royer and B. Remaud, *J. Phys. G* **10**, 1057 (1984).
- [10] G. Royer and J. Mignen, *J. Phys. G* **18**, 1781 (1992).
- [11] G. Royer and F. Haddad, *Phys. Rev. C* **47**, 1302 (1993).
- [12] H. J. Krappe, J. R. Nix, and A. J. Sierk, *Phys. Rev. C* **20**, 992 (1979).
- [13] A. J. Sierk, *Phys. Rev. Lett.* **55**, 582 (1985); *Phys. Rev. C* **33**, 2039 (1986).
- [14] S. Cohen, F. Plasil, and W. J. Swiatecki, *Ann. Phys. (N.Y.)* **82**, 557 (1974).
- [15] G. Royer and B. Remaud, *Nucl. Phys. A* **444**, 477 (1985).
- [16] W. J. Swiatecki, Lawrence Berkeley Laboratory Report No. 34928, 1993 (unpublished).